

## LEMMA approach for the production of low-emittance muon beams

N. AMAPANE<sup>(1)(2)</sup>, M. ANTONELLI<sup>(3)</sup>, F. ANULLI<sup>(4)</sup>, G. BALLERINI<sup>(8)(5)</sup>,  
L. BANDIERA<sup>(6)</sup>, N. BARTOSIK<sup>(2)</sup>, A. BERTOLIN<sup>(7)</sup>, C. BIINO<sup>(2)</sup>,  
O. R. BLANCO-GARCIA<sup>(3)</sup>, M. BOSCOLO<sup>(3)</sup>, C. BRIZZOLARI<sup>(8)(5)</sup>, A. CAPPATI<sup>(1)(2)</sup>,  
M. CASARSA<sup>(11)</sup>, G. CAVOTO<sup>(10)(4)</sup>, F. COLLAMATI<sup>(4)</sup>, G. COTTO<sup>(1)(2)</sup>,  
C. CURATOLO<sup>(7)</sup>, R. DI NARDO<sup>(12)</sup>, F. GONELLA<sup>(7)</sup>, S. HOH<sup>(9)(7)</sup>,  
M. IAFRATI<sup>(3)</sup>, F. IACOANGELI<sup>(4)</sup>, B. KIANI<sup>(2)</sup>, D. LUCCHESI<sup>(9)(7)</sup>,  
V. MASCAGNA<sup>(8)(5)</sup>, A. PACCAGNELLA<sup>(9)(7)</sup>, N. PASTRONE<sup>(2)</sup>, J. PAZZINI<sup>(9)(7)</sup>,  
M. PELLICIONI<sup>(2)</sup>, B. PONZIO<sup>(3)</sup>, M. PREST<sup>(8)(5)</sup>, M. RICCI<sup>(3)</sup>,  
S. ROSSIN<sup>(9)(7)</sup>, M. ROTONDO<sup>(3)</sup>, O. SANS PLANELL<sup>(1)(2)</sup>, L. SESTINI<sup>(7)</sup>,  
M. SOLDANI<sup>(8)(5)</sup>, A. TRIOSI<sup>(13)</sup> E. VALLAZZA<sup>(8)</sup> S. VENTURA<sup>(7)</sup>  
and M. ZANETTI<sup>(9)(7)</sup>

<sup>(1)</sup> *Università degli Studi di Torino - Torino, Italy*

<sup>(2)</sup> *INFN, Sezione di Torino - Torino, Italy*

<sup>(3)</sup> *INFN, Laboratori Nazionali di Frascati - Frascati, Italy*

<sup>(4)</sup> *INFN, Sezione di Roma - Rome, Italy*

<sup>(5)</sup> *Università degli Studi dell'Insubria - Como, Italy*

<sup>(6)</sup> *INFN, Sezione di Ferrara - Ferrara, Italy*

<sup>(7)</sup> *INFN, Sezione di Padova - Padova, Italy*

<sup>(8)</sup> *INFN, Sezione di Milano Bicocca - Milan, Italy*

<sup>(9)</sup> *Università di Padova - Padova, Italy*

<sup>(10)</sup> *Università di Roma La Sapienza - Rome, Italy*

<sup>(11)</sup> *INFN, Sezione di Trieste - Trieste, Italy*

<sup>(12)</sup> *CERN - Geneva, Switzerland*

<sup>(13)</sup> *Institut Pluridisciplinaire Hubert Curien - Strasbourg, France*

received 10 October 2019

**Summary.** — This work introduces an experimental test of the new proposal for a low-emittance muon accelerator (LEMMA). A low-emittance muon beam is obtained from the  $e^+e^- \rightarrow \mu^+\mu^-$  annihilation process at the threshold energy of 45 GeV eliminating the need for a dedicated muon cooling system. A series of two testbeam campaigns were carried out at CERN to validate this concept. The experimental setup is presented together with first preliminary results from the obtained data.

## 1. – Introduction to a Muon Collider

Active discussions are ongoing about the next possible accelerator that would best complement or even replace the LHC as the main instrument for consolidating the present knowledge of the Standard Model (SM) and searching for Beyond Standard Model (BSM) processes. The two most discussed classes of such accelerators are hadron-hadron and electron-positron colliders, possessing either very high centre-of-mass energy or very clean collision environment, respectively. Given that we still do not have clear evidences where new physics could be found, the ideal future discovery machine should possess both a high energy reach, for a direct observation of potential BSM particles, and the capability of high-precision measurements of SM processes, to find deviations from its predictions. An attractive solution in this scenario is a muon collider, which provides the same clean collision environment as electron-positron colliders, but thanks to the much smaller synchrotron radiation from muons allows to efficiently accelerate the beams to multi-TeV energies [1].

Studies of neutrino factories and muon colliders have been on-going since the 1990's in the USA within the Muon Accelerator Program (MAP) [2], where muons are produced through the decay of pions obtained from the collision of protons with a fixed target [3]. Muons that originate from pion decays at the material surface can be produced at a very high intensity, sufficient for a muon collider, but the resulting muon beams have very large emittance, which has to be reduced before accelerating the beams to collision energy. Therefore, a dedicated muon cooling section is foreseen as an intermediate step in the MAP accelerator concept, where emittance in the longitudinal and transverse planes is reduced to achieve sufficient luminosity, as shown in fig. 1. The ionisation cooling concept in the transverse plane has been tested by the MICE experiment at the Rutherford Appleton Laboratory, finishing its program with positive results which are now public [4]. The longitudinal cooling has not been put to test yet.

## 2. – LEMMA concept

The Low EMittance Muon Accelerator (LEMMA) program [6] is studying the possibility of a muon collider with performance similar to that of MAP, but with muon beams produced already with small emittance, eliminating the need for a complex and expensive ionisation cooling system. In this scheme muons are produced from annihilation of a high intensity positron beam with electrons in a fixed target at the centre-of-mass energy of the  $e^+e^- \rightarrow \mu^+\mu^-$  production threshold, which corresponds to a positron beam energy

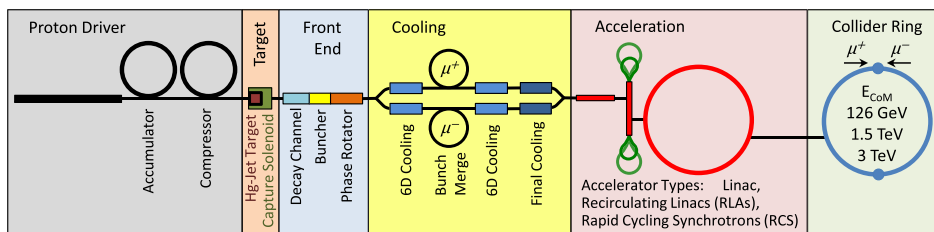


Fig. 1. – MAP accelerator concept. The proton beam interacts with the target to produce muons, which are then cooled by a sequence of passive absorbers and reaccelerated to recover the lost longitudinal momentum.

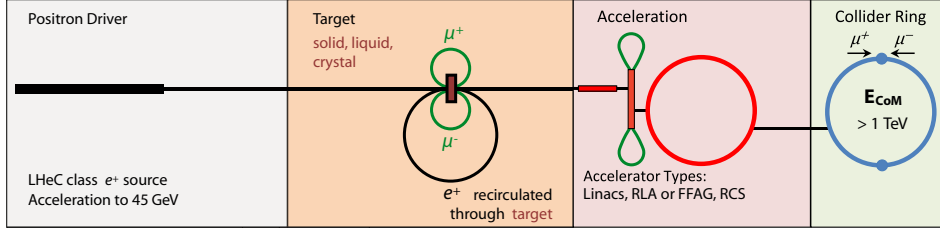


Fig. 2. – LEMMA accelerator concept. The beam in the positron ring (in black) interacts with the target on every turn. Muons are accumulated in the accumulator rings (in green) during less than one lifetime and then extracted for further acceleration.

of 45 GeV [5]. The schematic design of the LEMMA scheme is shown in fig. 2.

A number of challenges have to be addressed before making the LEMMA concept applicable in a real Muon Collider. First, the muon production rate is limited by the small cross section of the  $e^+e^- \rightarrow \mu^+\mu^-$  process: 0.1 to 1  $\mu\text{barn}$ . This implies that a very high flux of positrons is required to obtain a sufficient number of muons. A potential solution to this issue consist in recirculating the positron beam through the target in a 6.3 km long ring, as shown in fig. 2. The produced muons are stored in the two accumulator rings before being extracted for further acceleration.

A second challenge of the LEMMA scheme is the thermo-mechanical stress in the target material caused by the absorption of a high-intensity positron beam. Among several target options that are currently under consideration, a solid beryllium (Be) target is the primary candidate providing a good balance between the muon production rate and degradation of the positron beam.

After demonstrating with initial simulation studies that the beam emittance can be kept under control in the whole accelerator chain [6, 7], LEMMA has started to move towards experimental validation of the low emittance muon production concept. In total two testbeam campaigns were carried out at the CERN North Area using positrons from the H4 beam line in 2017 and from the H1 beam line in 2018. In the following the latest experimental setup, 2018, is described as well as a first evaluation of its performance is given.

### 3. – Experimental setup

The experimental setup was designed to measure with high precision trajectories and momenta of the two final state muons as well as direction of the incoming positrons. The layout of the setup is schematically shown in fig. 3, with the right-handed coordinate system defined by the Z axis pointing in the direction of the positron beam, the Y axis pointing to the roof of the experimental hall and the X axis orthogonal to the other two axes. The positron beam is passing through a plastic scintillator and a pair of silicon tracking sensors before hitting the target. This allows to measure the direction and position of the positron beam on the target. The silicon sensors are  $1.9 \times 1.9 \text{ cm}^2$  in size and provide position measurements with a microstrip pitch of  $50 \mu\text{m}$  [8]. Muon pairs produced in the target material pass through the vacuum beam pipe and another pair of silicon sensors, one before and one after the pipe, which measure the direction of the muons before passing through the 2 T magnetic field created by a dipole magnet.

Downstream of the magnet the paths of the muons diverge into two arms. Momenta

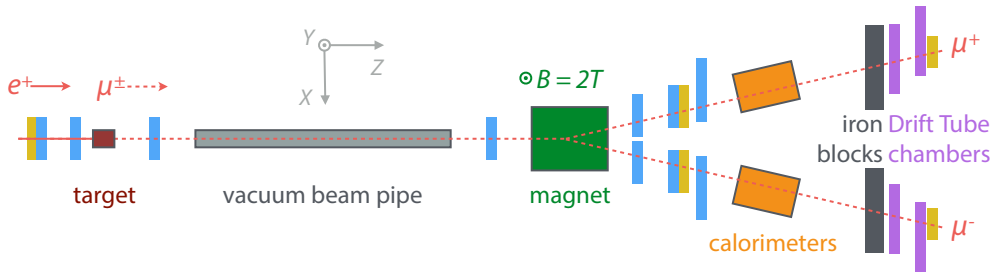


Fig. 3. – Schematic view of the LEMMA experimental setup as used in the testbeam of August-September 2018. All the components of the setup are marked in the figure except for a sequence of silicon tracking sensors (in blue) and plastic scintillators (in yellow) that were used to trigger the data acquisition.

can be reconstructed using measurements upstream and downstream of the bending magnet. In each arm a muon passes through three layers of silicon sensors followed by a calorimeter and by two layers of Drift Tube (DT) muon chambers. Silicon microstrip sensors positioned downstream of the target vary in size from  $9.5 \times 9.5 \text{ cm}^2$  closer to the target to  $18 \times 18 \text{ cm}^2$  in front of the DT chambers, with a spatial resolution ranging from  $228 \mu\text{m}$  in the smaller sensors to  $456 \mu\text{m}$  in the larger ones [9]. All silicon modules provide measurements both along the X and Y axes. The DT chambers consist of four layers of wires each, providing up to 8 hits in the Z-X plane in each arm. The expected spatial resolution along the X axis is about  $150 \mu\text{m}$ .

Positrons are expected to deposit most of their energy in the calorimeter. Any eventual leakage being absorbed by the iron shielding placed downstream such that only  $\mu^\pm$  tracks were expected to reach the DT chambers. Each calorimeter consists of a lead-glass ( $\text{PbWO}_4$ ) section followed by a Cherenkov section, to differentiate between electron and muon tracks.

Finally a pair of plastic scintillators positioned after the 2nd Si layer and behind the last DT chamber in each arm serve as a trigger for the data acquisition system (DAQ) requiring a coincidence between signals from all the scintillators in both arms and the scintillator at the positron entry point. The trigger signal was used to acquire data from the silicon sensors and the calorimeters, while the DT chambers were using a completely independent trigger-less readout system, which periodically acquired all chambers every 25 ns. The trigger signal from the scintillators was shared between the two DAQ systems for synchronisation and offline event building.

#### 4. – Analysis strategy

At the beginning of each test beam campaign series of calibration runs were recorded in different configurations. In particular during the last campaign of September 2018 the following calibration runs were recorded:

- $e^+$  beam at energies in range 16-28 GeV in steps of 2 GeV without target: for alignment of the silicon modules and calibration of the calorimeters;
- same configuration but with a reversed magnetic field direction to obtain signals in the other arm of the setup;

TABLE I. – *Configurations of physics runs taken with the positron beam and cylindrical targets during the testbeam campaign of September 2018.*

$e^+$ energy, GeV	Target material	Length, mm	Diameter, mm
45.0	Be	60	40
46.5	Be	60	40
49.0	Be	60	40
45.0	C	60	40
45.0	C	20	40

- $\mu^+$  beam at energies of 22 GeV, 26 GeV and 30 GeV, without target and with both magnetic field directions: for alignment of the calorimeters and DT muon chambers.

The calibration runs with positron beams were also used to ensure that no tracks were registered by the DT chambers, which was confirmed by the analysis of the recorded data.

Physics runs were recorded with the positron beam impinging on a cylindrical target in different configurations, varying the positron beam energy as well as target material and dimensions, as summarised in table I.

The process of interest is  $e^+e^- \rightarrow \mu^+\mu^-$  which implies the presence of two reconstructed muon tracks in the DT chambers and silicon modules. The reconstruction starts from the hits in the muon chambers that are fitted by straight lines and then propagated downstream, towards the silicon detectors. A similar fit procedure is applied to the 3 silicon detectors of each arm. Matching segments in silicon modules and DT chambers are retained. A first assumption about the muon momenta is also obtained. It is then used to propagate the track to the first silicon detector upstream of the magnet, with a circular track model. A linear extrapolation is then used to propagate the tracks to the silicon module next to the target. Finally all hits are fitted again to obtain the best estimate of the track momenta and angle in the bending plane, X-Z. Candidate events are selected if both  $\mu^+$  and  $\mu^-$  track fits converged.

## 5. – Results

Following the reconstruction procedure described in the previous section, a distribution of hit positions in the silicon modules before and after the vacuum beam pipe was obtained, as shown in fig. 4. Comparison with a Monte Carlo (MC) simulation shows reasonable agreement. The larger width of the hits position distribution in data w.r.t MC in the silicon detector upstream of the beampipe is primarily caused by a simplified distribution of the muon origin used in the simulation, which covers a smaller region than in the real target. This effect is not visible anymore in silicon module further away from the target, where the effect of the muon origin is much less relevant. The MC simulation can be further refined to take into account similar effects neglected at present.

The reconstructed momenta of the muon tracks were also used to calculate the invariant mass of the muon pairs,  $m_{\mu^+\mu^-}$ , as shown in fig. 5. Minor discrepancies in the shapes of the distributions are expected to come primarily from the misalignment of the experimental setup, which will be further corrected for at the later stage of the analysis.

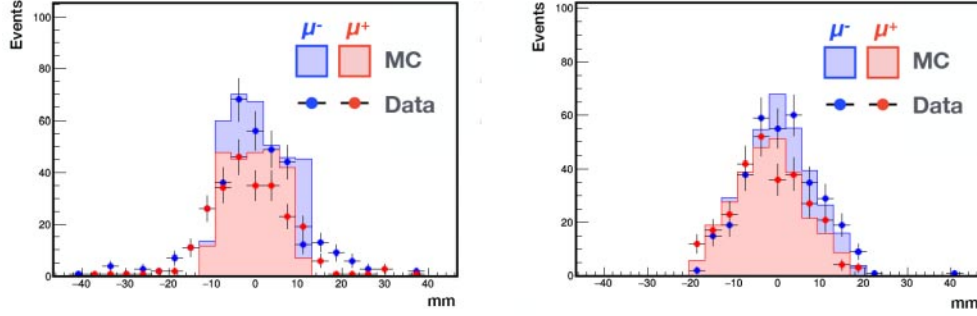


Fig. 4. – Hit positions from reconstructed  $\mu^+$  and  $\mu^-$  tracks measured in the silicon modules upstream (left) and downstream (right) of the vacuum beam pipe. MC distributions were obtained by generating muon pairs with a flat distribution along the Z axis within the target region and along the X axis within the  $[-10, 10]$  mm region.

## 6. – Trigger efficiency

Thanks to the fact that the muon chambers are using an independent trigger-less readout system, running at 40 MHz (25 ns), it is possible to estimate the efficiency of the external trigger used by the global DAQ. Every hit registered by the DT DAQ has a timestamp: the time when the charge carriers reach the corresponding wire. To convert such a timestamp to a distance of the hit from the corresponding wire it is necessary to know the timestamp of the actual event, which is normally provided by the external trigger. But the special arrangement of wires, in staggered layers, inside a DT chamber allows to independently measure the timestamp of such events by looking for specific 3-hit patterns, using the so called meantimer method [10]. A preliminary estimate from the September 2018 testbeam data showed that the trigger efficiency varied from about 2% at the beginning of data taking up to 20% once hardware issues with the trigger were identified and solved.

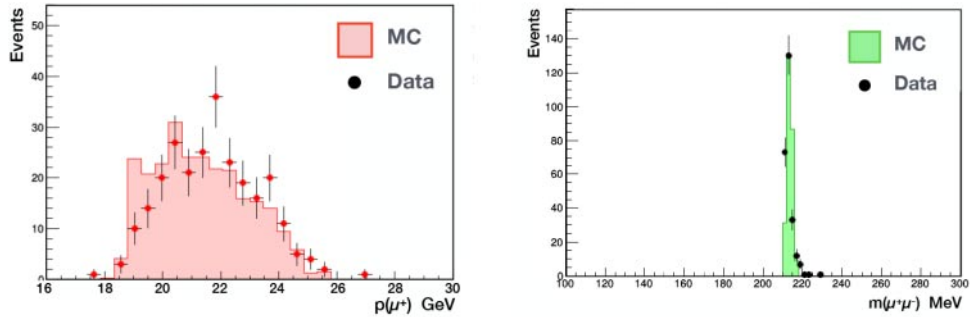


Fig. 5. – Reconstructed momentum of the positively charged muon track (left) and invariant mass of the reconstructed muon pair (right) compared to the corresponding distributions simulated with MC.

## 7. – Conclusions

While a Muon Collider is a very promising option for a future high-energy collider, this option has a number of challenges, one of which is the production of muon beams with very low emittance. For the first time the LEMMA concept has been implemented experimentally with a setup that should allow to measure the resulting beam emittance with different positron beam energies and targets. A very preliminary analysis of the experimental data already shows an encouraging and reasonable agreement with MC simulations, while there is still a lot of room for improvements in terms of detector alignment and calibrations. It was also confirmed that the trigger efficiency can be determined using the DT data.

\* \* \*

One of the authors (FI) acknowledges the support of CRYSBEAM project GAn. 615089.

## REFERENCES

- [1] ZIMMERMANN F., *Nucl. Instrum. Methods A*, **909** (2018) 33 arXiv:1801.03170.
- [2] RYNE R. D. *et al.*, *Design concept for muon-based accelerators*, WEPWA057, in *Proceedings of IPAC 2015, Richmond, VA, USA*.
- [3] BERG F., *Development of a next-generation high-intensity muon beam at the Paul Scherrer*, LNF Mini-Workshop Series: Muon production and beam interceptors, April 19, 2018, LNF/INFN, Frascati, Italy.
- [4] MOHAYAI T. A. *et al.*, *First demonstration of ionization cooling in MICE*, FRXGBE3, in *Proceedings of IPAC 2018, Vancouver, BC, Canada*.
- [5] ANTONELLI M. *et al.*, *Nucl. Instrum. Methods A*, **807** (2015) 101.
- [6] BOSCOLO M. *et al.*, *Phys. Rev. Accel. Beams*, **21** (2018) 061005.
- [7] ALESINI D. *et al.*, *Positron driven muon source for a muon collider*, arXiv:1905.05747.
- [8] LIETTI D. *et al.*, *Nucl. Instrum. Methods A*, **729** (2013) 527.
- [9] BARBIELLINI G. *et al.*, *Nucl. Instrum. Methods A*, **490** (2002) 146.
- [10] RD5 COLLABORATION *et al.*, *Nucl. Instrum. Methods A*, **336** (1993) 91.